INTERGRANULAR FRACTURE AT ELEVATED TEMPERATURE*

RISHI RAJ† and M. F. ASHBY‡

The kinetic problem of intergranular fracture at elevated temperatures by the nucleation and growth of voids in the grain boundary is analysed in detail. Diffusional transport accounts for the void growth-rate in the analysis, and the nucleation-rate is obtained by using the concepts of classical nucleation theory. The two are compounded to calculate the time-to-fracture. The influence of grain size, strain-rate, temperature, second phase particles and interface energies is taken into account. Particular attention is given to the presence of inclusions in the boundary; the role of the stress concentration at the interface between the inclusion and the matrix, and the energy of this interface is investigated.

RUPTURE INTERGRANULAIRE AUX TEMPERATURES ELEVEES

On analyse en détail le problème cinétique de la rupture intergranulaire aux températures élevées par la germination et la croissance de cavités aux joints de grains. Dans cette analyse, le transport de matière par diffusion rend compte de la vitesse de croissance des cavités, et l'on obtient la vitesse de germination en utilisant les concepts de la théorie classique de la germination. On combine croissance et germination pour calculer le temps jusqu'à rupture. On tient compte de l'influence de la taille des grains, de la vitesse de déformation, de la température, de particules d'une seconde phase et des énergies d'inter-face. On insiste en particulier sur la présence d'inclusions dans les joints. On étudie le rôle de la con-centration de contraintes à l'interface inclusion-matrice, et de l'énergie de cet interface.

INTERGRANULARER BRUCH BEI HÖHEREN TEMPERATUREN

Das Kinetikproblem des intergranularen Bruchs bei höheren Temperaturen durch Keimbildung und Wachstum von Hohlräumen in der Korngrenze wird ausführlich untersucht. Die Analyse zeigt, daß Diffu-sionstransport zum Wachstum der Hohlräume führt und daß die Keimbildungsgeschwindigkeit mit dem Konzept der klassischen Keimbildungstheorie gewonnen werden kann. Aus beiden wird die Zeit bis zum Bruch berechnet. Der Einfluß von Korngröße, Abgleitgeschwindigkeit, Temperatur, Teilchen der zweiten Phase und Grenzflächenenergien wird berücksichtigt. Insbesondere wird die Gegenwart von Einschlüssen in der Korngrenze betrachtet. Die Rolle der Spannungskonzentration an der Grenzfläche zwischen Einschluß und Matrix und die Energie dieser Grenzfläche werden untersucht.

1. INTRODUCTION

Fracture of polycrystalline solids under creep con-ditions can be caused by the growth and coalescence of voids on the grain boundaries. Under the right con-ditions, the voids grow by the diffusive motion of vacancies to them.[1] The same fracture mechanism has been held responsible for the minimum in time-to-fracture, or in the ductility, sometimes observed when polycrystals are pulled in tension at a constant rate.[2,3] The diffusional growth of voids has been analysed by Speight and Harris[4] and earlier by Hull and Rimmer,[5] and is (at least partly) explained. Their nucleation, on the other hand, is still not completely understood: measurements of their nucleation-rate, for instance, are inconclusive.[1,6] It has been suggested that stress concentrations at inclusions and triple points can lead to void nucleation.[7]

An analysis is presented here which envelopes many of the aspects of intergranular fracture mentioned above and which can be used to calculate the time to fracture for a given grain size, strain-rate, temperature, size and density of second phase particles in the bound-ary, and the various interface energies. It uses a unified approach whereby different void configurations (at least five are possible) can be dealt with simultane-ously. We first calculate the time-to-fracture when a fixed number of pre-existing voids is present. Next we apply classical nucleation theory to the nucleation-rate of the voids on non-sliding boundaries and on boundaries which slide. The growth-rate and the nucleation-rate are then compounded, using a numeri-cal method, to calculate the time-to-fracture.

Sliding at a grain boundary which contains in-clusions can concentrate the tensile stress at the inter-face at which the inclusion and the matrix meet. We calculate this interface stress (using an upper bound criterion) and the new nucleation rate and time-to-rupture. The combination of the stress concentration and the high interface energy at an inclusion makes it a probable site for void nucleation. The calculations lead to the conclusion that inclusions should be largely responsible for intergranular fracture at elevated tem-peratures in polycrystals, and predict the influence of grain size, inclusion size and density, and strain-rate on the ductility of polycrystals.

The notation used in this paper is summarized in Table 1.

2. VOID GEOMETRIES

Voids formed at the grain boundaries can have differ-ent shapes depending on whether they are formed at two-grain junctions, three-grain junctions, four-grain junctions or at the interface of inclusions present in
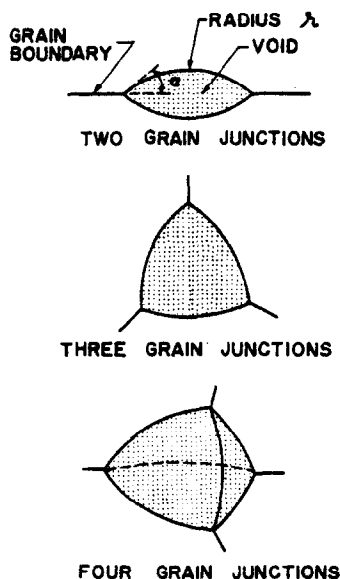
1

FIG. 1. Void geometries in inclusion free grain boundaries.

the grain boundaries. All voids, however, have two features in common: the free surfaces of the voids are spherical segments (provided that surface diffusion is rapid enough to maintain the uniform curvature† as the void grows) and the angles formed between the void and the interfaces which contain it must be such as to satisfy equilibrium between the surface tension forces in question. The voids considered in this paper fall into two categories: voids formed in inclusion-free grain boundaries; and voids formed in boundaries which contain inclusions.

2.1 Voids in inclusion-free boundaries

Figure 1 shows the shapes of voids at two-grain junctions, three-grain junctions and four-grain junctions. The geometry of these voids is described by the radius of the void surface, r, and the angle α formed at the junction of the void and the grain boundary. This angle is dictated by equilibrium between surface tension forces at the junction, so that:

$$\alpha = \cos^{-1}\left(\frac{\gamma_B}{2\gamma}\right) \tag{1}$$

where γ_B is the energy (per unit area) of the grain boundary and γ is the energy of the free surface of the void. (Typically for clean surfaces in pure metals, $\gamma_B \approx \gamma/2$ and $\alpha \approx 75°$.)

---

† This is not always true. Under conditions that cause a void to grow rapidly, matter is removed from its perifery by grain boundary diffusion faster than surface diffusion can redistribute matter on the void surface. It will then become increasingly penny-shaped, and spread in the boundary plane faster than calculated here. For simplicity we neglect this effect.

Three geometric properties of the void—its volume V, its free surface area S and the grain boundary area B that it replaces—can be expressed as functions of r and x. In general:

$$V = r^3 F_V(\alpha) \tag{2a}$$

$$S = r^2 F_S(\alpha) \tag{2b}$$

$$B = r^2 F_B(\alpha). \tag{2c}$$

The functions of α depend on the void type. They have been calculated[8] and are quoted in Appendix I for three- and four-grain junctions. For two-grain junctions they are:

$$F_V(\alpha) = \frac{2\pi}{3}(2 - 3\cos\alpha + \cos^3\alpha) \tag{3a}$$

$$F_S(\alpha) = 4\pi(1 - \cos\alpha) \tag{3b}$$

$$F_B(\alpha) = \pi\sin^2\alpha. \tag{3c}$$

Note that as α increases to $\pi/2$, equations (2 and 3) give the properties of a sphere. Remembering that the radius of the circle of intersection of the void with the boundary is $r_B = r\sin\alpha$ it can be seen that, as α decreases to zero, equations (2 and 3) give the properties of a penny-shaped disc.

2.2 Voids formed at inclusions

Figure 2 shows that two types of voids can form at inclusions. One lies completely on the inclusion-matrix interface (Type A), and the other extends into the grain boundary (Type B). Two new angles, β and
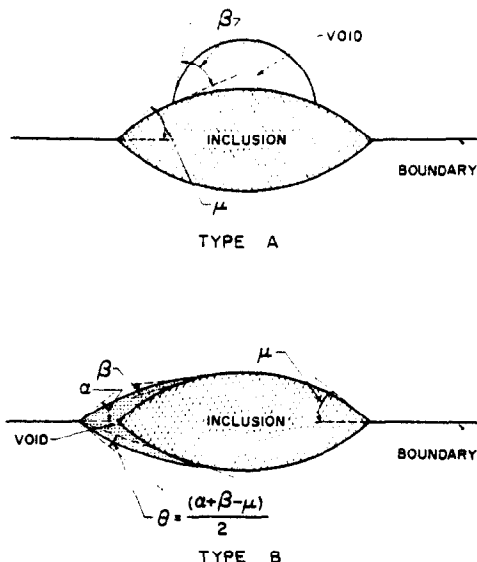

FIG. 2. Two types of voids which can form at inclusions present in a grain bondary.

μ are needed to describe them. They are shown in Fig. 2 and satisfy the following interface energy relationships:

$$\beta = \cos^{-1}\left\{\frac{\gamma_{IB} - \gamma_I}{\gamma}\right\} \qquad (4)$$

and

$$\mu = \cos^{-1}\left\{\frac{\gamma_B}{2\gamma_{IB}}\right\}. \qquad (5)$$

where γ_I is the energy of the inclusion free surface and γ_{IB} is the energy of the inclusion-matrix interface.

The geometrical properties of the Type A void are given to a good approximation (provided the void is small compared with the inclusion) by equation (2) and the following angle functions:

$$F_\Gamma = \frac{\pi}{3}(2 - 3\cos\beta + \cos^3\beta) \qquad (6a)$$

$$F_S = 2\pi(1 - \cos\beta) \qquad (6b)$$

$$F_B = \pi\sin^2\beta. \qquad (6c)$$

The properties of the Type B voids are more difficult to calculate. The exact calculation is given in Appendix I but approximately (to within a factor of two) the volume is given by:

$$V = r^3 \frac{4\pi}{3}\left[2 - 3\cos\left(\frac{\alpha + \beta - \mu}{2}\right) + \cos^3\left(\frac{\alpha + \beta - \mu}{2}\right)\right]. \qquad (7)$$

The reason for this approximation is evident by inspection of Fig. 2.

In the calculations to follow, we shall use the expressions in equations (1–7) and the equations in Appendix I.

3. TIME TO FRACTURE: FIXED NUMBER OF NUCLEI

In this section we assume that a fixed number of void nuclei exist, and can grow, as soon as a stress is applied to the hot specimen; and we calculate the time-to-rupture. For this purpose we consider a periodic array of voids in a grain boundary across which a tensile stress σ_∞ is applied. Voids will grow in volume by the diffusion of matter from the void surface into the grain boundary adjacent to the voids as shown in Fig. 3.

Diffusion occurs through the boundary and through the lattice. The steady-state growth of voids by boundary diffusion has been calculated by Hull and Rimmer[5] and Speight and Harris.[4] Though these solutions are a tolerable approximation for a wide
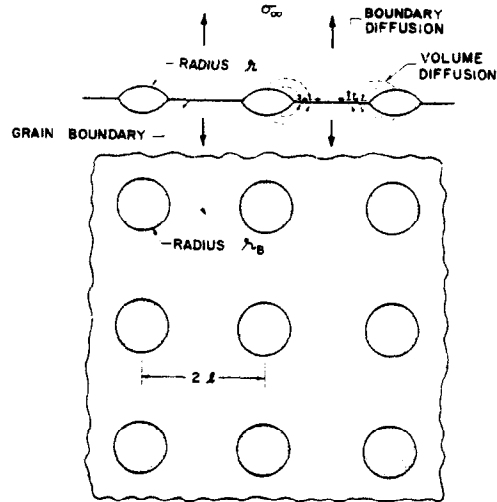

FIG. 3. A periodic array of voids in a grain boundary. A tensile stress of σ_∞ is applied normal to the boundary.

range of void sizes and stresses, they are not strictly correct because they used wrong boundary conditions in solving the diffusion equation.

A calculation that avoids this error is given in Appendix II. The rate-of-growth of the volume of voids which project a circular cross-section of radius r_B in the grain boundary and are spaced an average distance $2l$ apart, when growth is by boundary diffusion, is:

$$\left(\frac{dV}{dt}\right)_B = 2\pi\Omega\frac{D_B\delta}{kT}\left(1 - \frac{r_B^2}{l^2}\right)$$

$$\times \left[\frac{\left(\sigma_\infty - \frac{2\gamma}{r}\right)\left(1 - \frac{r_B^2}{l^2}\right)}{\log_e\left(\frac{l}{r_B}\right) - \frac{3}{4} + \frac{r_B^2}{l^2}\left(1 - \frac{r_B^2}{4l^2}\right)}\right], \qquad (8)$$

where r is the radius of curvature of the void surface, Ω is the atomic volume and $D_B\delta$ is the boundary diffusion coefficient times the boundary thickness. The equivalent solution for the volume diffusion case is obtained by making the usual approximation:[9]

$$\left(\frac{dV}{dt}\right)_{\text{vol. diff.}} = \left(\frac{dV}{dt}\right)_B\frac{2lD_v}{\pi\delta D_B}. \qquad (9)$$

This contribution is added to that given by equation (8) to give the total growth-rate of a void. In practice it is seldom the dominant contribution.

To calculate the time to fracture we define the area-fraction of voids in a grain boundary, $A(t)$, as:

$$A(t) = \frac{r_B^2}{l^2}. \qquad (10)$$

It is a measure of the damage to the material; that is, extent to which separation has progressed.

Rupture takes place after an elapsed time t_r when A reaches a final value A_r, which we will take to be 0.5. In any real material, holes will nucleate and grow, slowly at first, and then more rapidly as the local load-bearing cross-section is eaten away and the local stress rises. The final fracture must involve the tearing or rapid plastic deformation of the ligaments between the voids; but because hole growth in this final phase is rapid by any mechanism, it occupies only a small part of the life, and we ignore it in calculating t_r.

The time to fracture, t_r, has been derived in Appendix II:

$$t_r = \frac{3\sqrt{\pi}}{32} \frac{kT}{\Omega D_B \delta} \frac{1}{\sigma_\infty \rho^{3/2}} \frac{F_V(\alpha)}{F_B^{3/2}(\alpha)} \int_{A_{\min}}^{A_{\max}} \frac{dA}{f(A)} \quad (11)$$

where ρ is the number of voids per unit area of the boundary.

The integral in equation (11) is defined by equation (A2.12). Its value is 0.06 as shown in Fig. A2.1 and as explained in Appendix II. The value of the integral is insensitive to $A_{\max}$ when $A_{\max} > 0.1$ and changes very rapidly for $A_{\max} < 0.1$, implying that most of t_r is spent in the early stages of void growth.

The dependence of t_r on the shape functions $F_V/F_B^{3/2}$ is shown in Fig. 4. It increases almost linearly with α. Note that thin penny-shaped voids can be approximated by a small α while nearly spherical voids by a large α.

For boundary diffusion t_r varies as $1/\rho^{3/2}$. If the voids were growing by volume diffusion then, in view of equation (9), t_r would vary as $1/\rho$. The time to fracture, normalized with respect to the stress, is plotted in Fig. 5. (The physical constants for copper used in the calculation are given in the Nomenclature: α was taken to be $\pi/3$.) Note that volume diffusion dominates only when void densities are less than
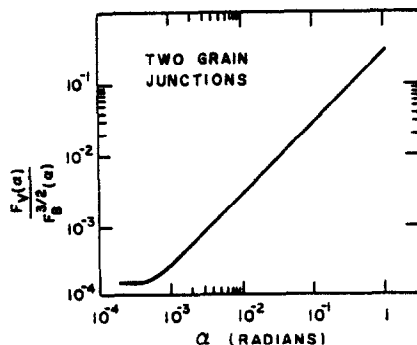

FIG. 4. Dependence of time-to-fracture upon α for two grain junctions for a fixed number of nuclei.
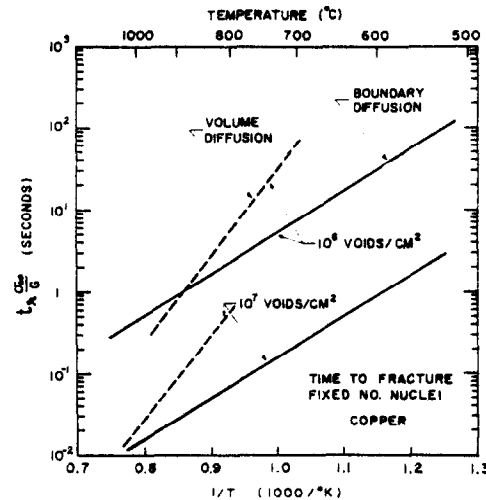

FIG. 5. Variation of time-to-fracture with temperature for a fixed number of nuclei. G is the shear modulus. The data is for copper (Nomenclature).

10^6 voids/cm². Typically, at a stress $\sigma_\infty = 10^{-4} G$, at 700°C and for a void density of 10^6 voids/cm² fracture would occur in one day.

4. NUCLEATION OF VOIDS

In contrast to the last section, we here assume that no voids exist in the virgin specimen, but that they must first be nucleated before they can grow. For this purpose we consider the nucleation of a void in a grain boundary across which a tensile stress σ_n acts. The factors contributing to the change in free energy of the system as a result of forming one void nucleus are: (a) the work done by the system on its surroundings, (b) change in the interface area—and thus energy—within the system and (c) change in the stored elastic energy in the system. Since the term (a) is of order σ_n and the term (c) is of order $\sigma_n^2/2E$, and since $E \gg \sigma_n$, term (c) may be neglected in comparison with (a). Recalling equations (2) we get the change in free energy:

$$\Delta G = -r^3 F_v(\alpha)\sigma_n + r^2[\gamma F_S(\alpha) - \gamma_B F_B(\alpha)]. \quad (12)$$

The critical radius, r_c, at which ΔG reaches a maximum, and the magnitude of this maximum, ΔG_c, can be calculated using equations (12, 2 and 3) and the equations in Appendix I. The result is a general one and is applicable to all types of void configurations:

$$r_c = \frac{2\gamma}{\sigma_n} \quad (13)$$

and

$$\Delta G_c = \frac{r_c^3 F_v(\alpha)\sigma_n}{2}. \quad (14)$$

Alternatively ΔG_c can be written as

$$\Delta G_c = \frac{(\text{Volume of the void of critical size}) \times \sigma_n}{2}. \quad (15)$$

If $\rho_{\max}$ is the maximum number of potential nucleation sites in the grain boundary per unit area, then the number of critical nuclei per unit area is

$$\rho_c = \rho_{\max} \exp\left(-\frac{\Delta G_c}{kT}\right). \quad (16)$$

The number of supercritical nuclei formed per second is ρ_c times the time-dependent probability, p_t. of adding one vacancy to the critical nucleus. p_t can be derived from the jumping frequency of a vacancy, which is related to the boundary self diffusion coefficient, and from the probability of finding a vacancy at the perimeter of the nucleus of critical size:[10]†

$$p_t = \frac{4\pi\gamma}{\sigma_n\Omega} \frac{D_B\delta}{\Omega^{1\cdot3}} \exp\left(\sigma_n\Omega/kT\right). \quad (17)$$

Since usually $\sigma\Omega/kT \ll 1$, combining equations (13–17) leads to the nucleation rate:

$$\dot{\rho} = \frac{4\pi\gamma}{\Omega^{4/3}\sigma_n} D_B\delta\left(1 + \frac{\sigma_n\Omega}{kT}\right)(\rho_{\max} - \rho)$$

$$\times \exp\left[-\left(\frac{4\gamma^3 F_v(\alpha)}{\sigma_n{}^2 kT}\right)\right]. \quad (18)$$

The exponential factor above is the dominant influence in the temperature dependence of nucleation; $F_v(\alpha)$, γ and σ_n are, therefore, the critical parameters in determining the nucleation rate. Note that $F_v(\alpha) = 0$ if: $\alpha = 0$ at two grain junctions, $0 \leq \alpha \leq \pi/6$ at three grain junctions, and $0 \leq \alpha \leq \sin^{-1}(\frac{1}{3})$ at four grain junctions; at these values of α there is no kinetic barrier to nucleation. However, $F_v(\alpha)$ increases rapidly as α increases beyond these values.

5. TIME TO RUPTURE II: CONTINUOUS NUCLEATION, NO GRAIN-BOUNDARY SLIDING

The compound problem of nucleation and growth of voids is solved by combining equation (11) with (18) since ρ, the void density, now becomes time-dependent. The new equation for t_r is:

$$0.5 = \frac{32\sqrt{\pi}}{3} \frac{\Omega D_B\delta}{kT} \sigma_\infty \frac{F_B{}^{3\cdot2}(\alpha)}{F_v(\alpha)}$$

$$\int_0^{t_r} \int_{\Upsilon}^{t_r} \rho^{1/2}(t - \Upsilon)\,\dot{\rho}(\Upsilon)f(A(t - \Upsilon))\,dt\,d\Upsilon. \quad (19)$$

† This probability is the number of periferal atom sites $2\pi r_B\delta\Omega^{1/3}/\Omega$ times the probability $D_b/\Omega^{2/3}$ that one jumps away from the void. The factor $e^{\sigma_n\Omega/kT}$ allows for the change in vacancy concentration caused by the stress. In obtaining equation (17), we have approximated r_B by $r_c = 2\gamma/\sigma_n$.

The numerical procedure for solving for t_r in the above equation is described in Appendix III.

In this section we consider the case where the normal stress in the boundary which causes nucleation, σ_n (equation 18), is equal to the applied stress, σ_∞; no stress concentration occurs in the boundary as a result of grain boundary sliding, or as a result of a slip within a grain being obstructed by a boundary.

As an example, consider a copper polycrystal with a grain size of 10 μm, strained at a constant strain-rate of 10^{-4}/sec. At high temperatures, the polycrystal will flow predominantly by *power-law creep*, or (very close to its melting point) by *diffusional flow*. At lower temperatures its flow is predominantly by the *glide motion of dislocations*. The stress required for flow at a constant rate depends on the way in which the kinetics of the dominant mechanism depend on temperature, and thus varies in a complicated way with temperature. Its behaviour has been described, compared with experiment, and presented in deformation-mechanism diagrams, in earlier publications;[11,12] the stress required to maintain a strain-rate of 10^{-4}/sec in a copper polycrystal was calculated by the method, and using the data, given in these references. The result is shown in Fig. 6. This relationship between stress and temperature has been used to calculate the time-to-rupture for the five possible configurations. These time-to-rupture curves are shown in Figs. 7. All are calculated for a strain-rate of 10^{-4}/sec, a grain size of 10 μm, and an inclusion density of 10^{10}/m².

The important features of these curves are:

(a) Ductility minimum

All curves show a minimum time-to-fracture at an intermediate temperature. This is because the rate of fracture is proportional to the product of the nucleation-rate and the growth-rate of the voids. As the
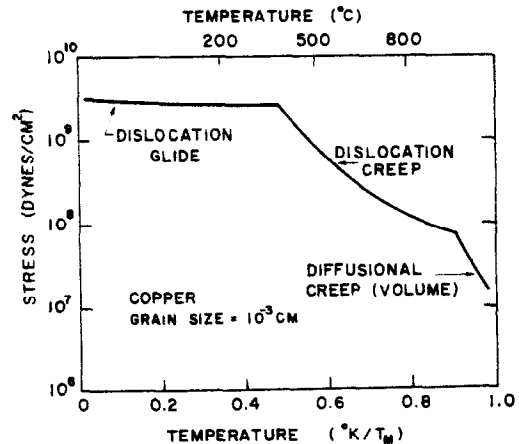

FIG. 6. Variation of stress with temperature when a polycrystal of copper of grain size 10 μm is strained at 10^{-4}/sec. Data from Refs. 11 and 12.

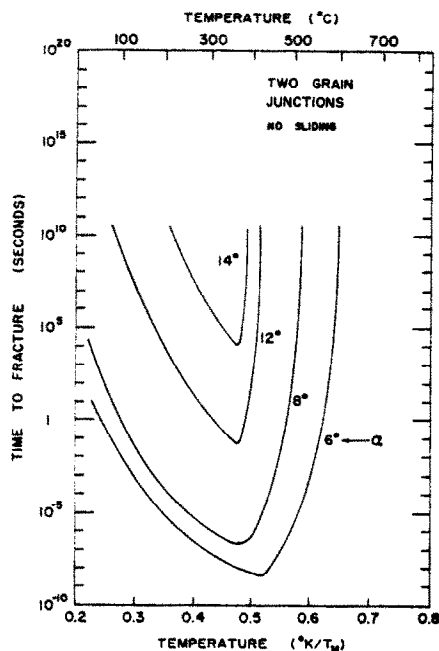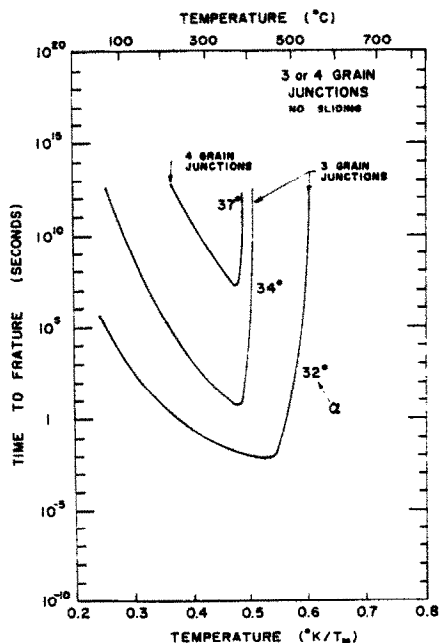FIG. 7(a). Void nucleation and growth at two grain junctions with no sliding.

FIG. 7(c). Void nucleation and growth at inclusions for Type A voids with no sliding.

FIG. 7(b). Void nucleation and growth at two, three and four grain junctions with no sliding.
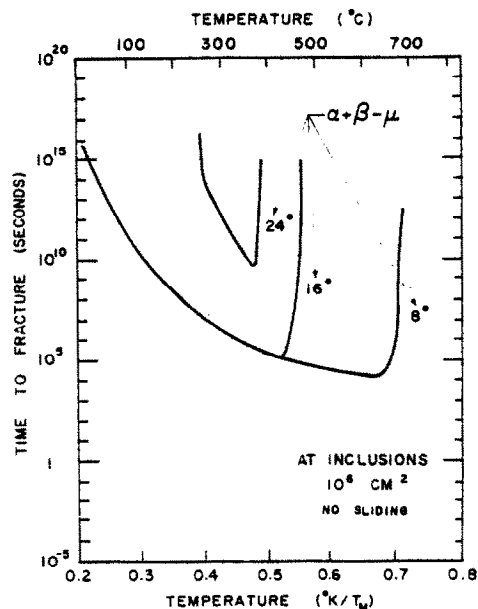
FIG. 7(d). Void nucleation and growth at inclusions for Type B voids with no sliding.

temperature increases, the stress required to maintain a given strain-rate falls in such a way that the growth rate increases, but the nucleation rate decreases. At low temperatures nucleation occurs readily, but the growth rate is small and determines the rupture life, whereas at high temperatures growth is fast and it is t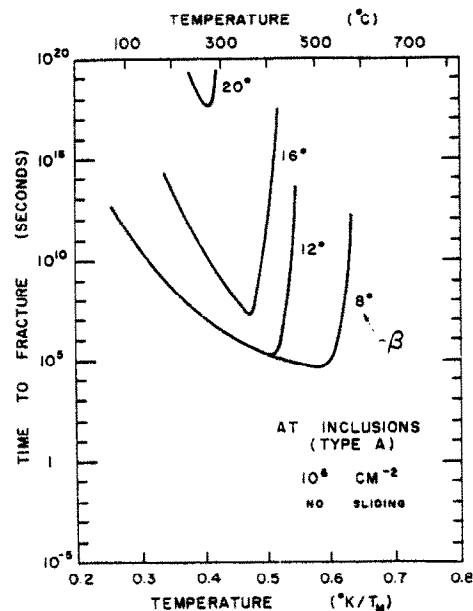he nucleation rate that is small, and determines the life. This results in a minimum value for t_r at an intermediate temperature. At temperatures above $0.7T_M$ nucleation often ceases completely, which precludes intergranular fracture. Note that the minimum moves to a lower temperature as α increases. The very sharp minimum is partly due to our assumption of a unique, uniform grain-size, and nucleus distribution, so that

all grains cavitate simultaneously and to the same extent. Any spread in these quantities broadens the minimum.

(b) Nucleation rate

When no grain boundary sliding is allowed. as in the present case, then, in general, nucleation is continuous with time i.e., the number of nuclei increases with time towards the number ρ_{max}.

(c) Sensitivity to α

α by its definition in equation (1) is the primary measure of the surface energy barrier to void nucleation. At two-grain junctions, for instance, the energy barrier to nucleation vanishes as α goes to zero. but grows, causing the nucleation rate to decrease rapidly, as α increases from 6 to 14° (Fig. 7a). For three- and four-grain junctions there is no barrier to nucleation when $\alpha = 30$ and 36° respectively. A slight increase in α above these limits causes a rapid change in nucleation rate as shown in Fig. 7(b) nucleation ceases when $\alpha = 37°$. Since for a pure metal, $\alpha \approx 75°$, no nucleation will occur unless inclusions are present in the boundaries.

(d) Type A and type B voids

For Type A voids at inclusions the angle β (Fig. 2) is the important surface energy parameter. Fracture is possible for $\beta < 20°$ as shown in Fig. 7(c). The parameter $(\alpha + \beta - \mu)$ as described in Fig. 2 and Section 1 is a measure of the surface energy barrier for Type B voids forming at inclusions. As shown in Fig. 7(d) fracture is possible if $(\alpha + \beta - \mu) < 24°$. In general, Type B nucleation sites will be favored when $\mu < \alpha$, i.e. when $\gamma_{IB} < \gamma$ (by consideration of equations (1 and 5).

6. TIME TO RUPTURE III: CONTINUOUS NUCLEATION, WITH SLIDING

6.1 Stress concentration at inclusions due to sliding

Sliding across an inclusion in a grain boundary must be accommodated.[9,13] If the sliding displacements are too large to be accommodated elastically, then accommodation must be by diffusional flow or plastic flow (Fig. 8). The upper bound for the steady-state
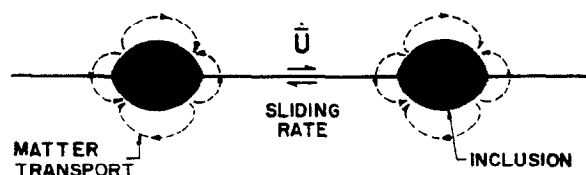

FIG. 8. Sliding across an inclusion must be accommodated by transport of matter.

stress† that can be maintained at an inclusion during creep is that required to drive the diffusive fluxes, either by lattice or by boundary diffusion, which will accommodate the incompatibility which appears there. Following a procedure described earlier[9] the normal traction at the interface, σ_n, can be calculated for an imposed sliding rate $\dot{U}$ at the boundary; typically its magnitude is (Ref. 9, Appendix B)

$$\sigma_n = \frac{kT}{1.6\Omega} \frac{p\dot{U}}{D_v\left(1 + \frac{5\delta D_B}{pD_v}\right)}, \qquad (20)$$

where p is the diameter of an inclusion. For a strain rate of $\dot{\varepsilon}$ and a grain size of d, the maximum possible sliding rate is

$$\dot{U} = \dot{\varepsilon}d \qquad (21)$$

Substituting this into equation (20) gives the upper bound for σ_n.

The time to fracture curves shown in Figs. 9(a and b) were evaluated by using this estimate of σ_n in equation (18 and 19).

6.2 Fracture curves for type A and type B voids

Fracture curves for Type A are given in Fig. 9(a) and for Type B voids in Fig. 9(b). Fracture is now possible
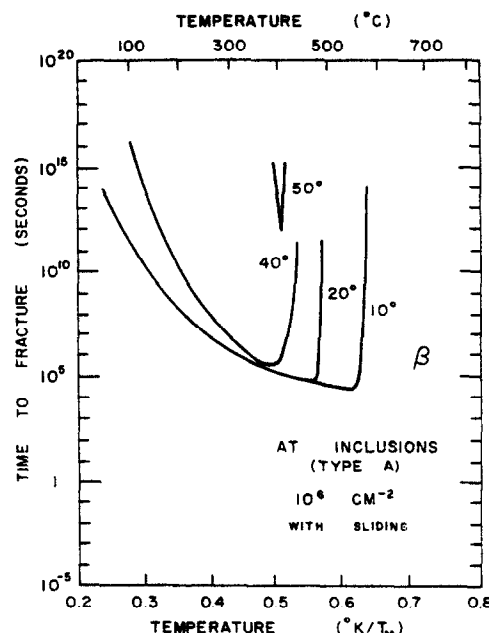

FIG. 9(a). Void nucleation and growth at inclusion for Type A voids with sliding.

---

† On initial loading, or when the stress is suddenly changed. much larger stresses can appear:[21] these relax to the value quoted above with a characteristic relaxation time; but during that time, nucleation may occur.
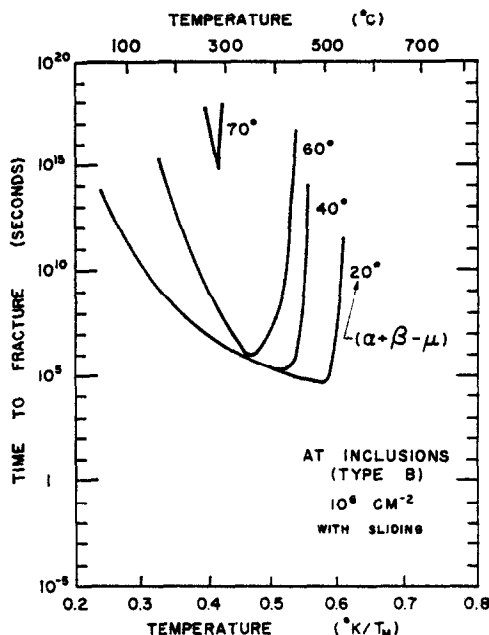
FIG. 9(b). Void nucleation and growth at inclusion for
Type B voids with sliding.

for $\beta < 40°$ and for $(\alpha + \beta - \mu) < 70°$. It becomes
easier to nucleate Type B voids than Type A voids.
The ductility minimum is observed in these curves for
the same reasons as before; and, as before, the mini-
mum moves to a lower temperature as the energy
angle is increased. The nucleation behaviour, however,
is different: instead of continuous nucleation we now
get catastrophic nucleation: full nucleation occurs
early in the fracture process. There are two reasons
for this: first the maximum number of nucleation
sites (equal to the number of inclusions) is fewer; and
second, σ_n varies more rapidly with temperature than
σ_∞ (at a constant strain-rate).

The value of the parameters used in the generation
of Figs. 9(a and b) were: inclusion size 1 μm, grain
size 10 μm, inclusion density 10^{10}/m², and strain-rate
10^{-4}/sec.

6.3 Sensitivity of fracture curves to different parameters

Figures 10–14 demonstrate the sensitivity of the
fracture curves to strain rate, grain size, particle size,
particle density and the distribution of particles. All
curves were plotted for $\alpha + \beta - \mu = 40°$ (except in
Fig. 10 where $\alpha + \beta - \mu = 20°$) and for $\alpha = 35°$, and
(except where otherwise noted) a strain-rate of 10^{-4}/
sec, a grain size of 10 μm, an inclusion density of
10^{10}/m² and an inclusion size of 1 μm. Stress con-
centration due to sliding was taken into account and
Type B void nucleation was considered. The relative

aspects of the results would have remained the same
if a different set of conditions had been chosen.

(i) *Strain-rate* (*Fig.* 10). As strain rate decreases
the minimum moves to a lower temperature and to a
higher value for time-to-fracture. For example. at a
strain rate of 10^{-4}/sec the minimum occurs at 0.58 T_M
and the time-to-fracture is 4.3×10^4 sec; at 10^{-6} sec
the values are $0.44T_M$ and 1.6×10^6 sec.
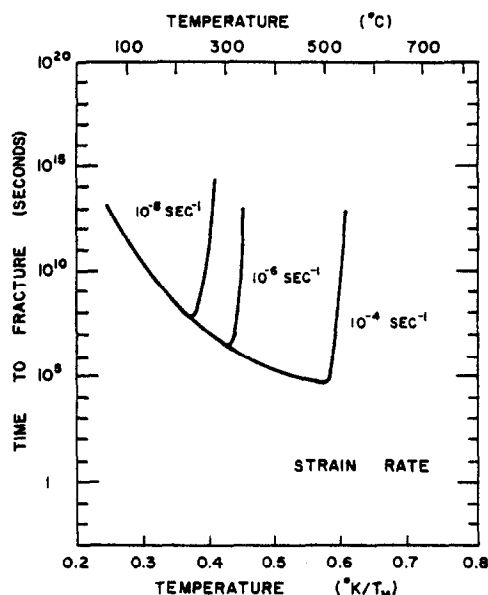

FIG. 10. The influence of strain rate on ductility. $\alpha + \beta - \mu = 20°$, Type B voids.

(ii) *Grain size* (*Fig.* 11). A smaller grain size im-
proves ductility; it moves the minimum to a lower
temperature and a higher value of time-to-fracture.
For example, for a grain size of 10 μm the minimum
occurs at 0.52 T_M and the time-to-fracture is $1.2 \times
10^5$ sec whereas for a grain size of 100 μm the values are
$0.62T_M$ and 2.4×10^4 sec. These conclusions are in
qualitative agreement with published experimental
work.[14,15]

(iii) *Inclusion size* (*Fig.* 12). A smaller particle size
improves ductility. For example for a particle size of
1 μm the minimum occurs at $0.52T_M$ and the time-
to-fracture is 1.2×10^5 sec whereas for a particle size
of 0.1 μm the values are $0.4T_M$ and 1.2×10^7 sec.

(iv) *Inclusion density* (*Fig.* 13). As expected from
equation (11) the time-to-rupture varies inversely as
the three-halves power of the number of inclusions per
unit area in the grain boundary.

(v) *Distribution of the second phase* (*Fig.* 14). Frac-
ture curves are shown when the distribution of the
second phase in the grain boundary changes although
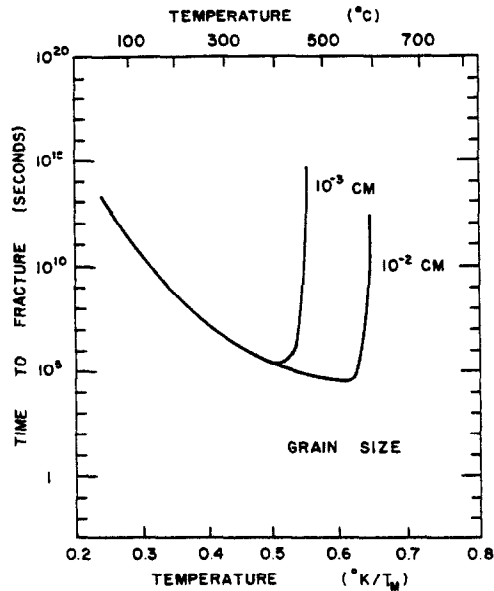its total volume fraction remains constant. A larger

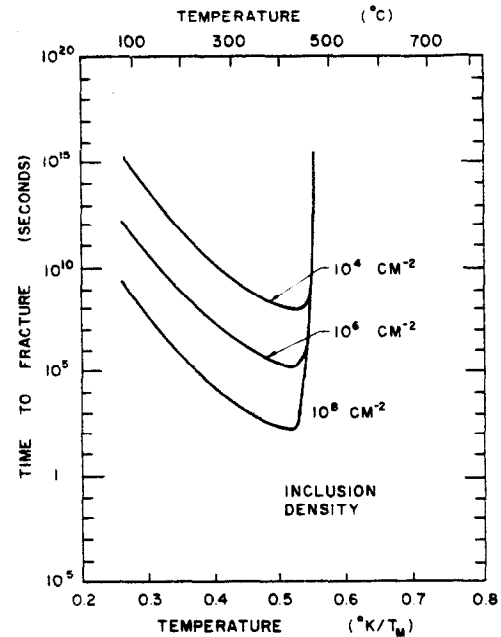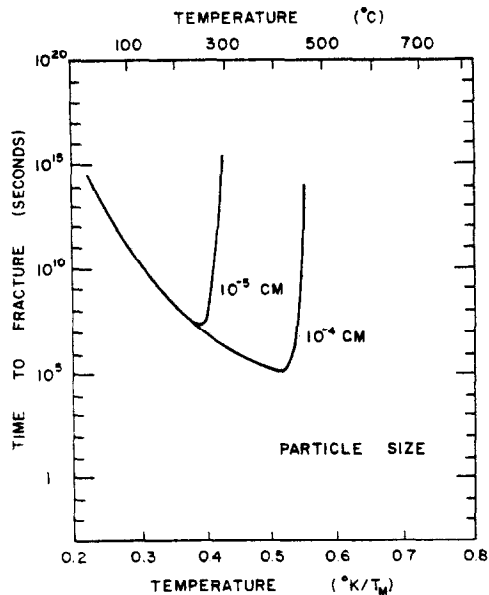Fig. 11. The influence of grain size on ductility. Type B voids.

Fig. 13. The influence of inclusion density on ductility. $\rho = 10^{-6}$ m. Type B voids.

Fig. 12. The influence of inclusion size on ductility. Type B voids.

Fig. 14. The influence of the dispersion of second with the total volume of the second phase remaining constant. Type B voids.

particle size moves the minimum to a higher temperature but also raises it to a higher value of time-to-fracture. For large particles the minimum occurs at $0.6T_M$ and 3.4×10^4 sec while for the small particles it occurs at $0.44T_M$ and 1.6×10^3 sec.

6.4 The role of interface energies

It has been shown that the nucleation of voids is sensitive to the energy angle β for Type A voids and to

$(\alpha + \beta - \mu)$ for Type B voids. The dependence of these angles on interface energies has been described in Section 2. Four interfacial energies are involved: γ and γ_I. the matrix free surface and the inculusion free surface energy; and γ_B and γ_{IB}, the grain boundary interface and the inclusion-matrix interface energy. As an example, consider the case of grain boundaries in copper containing silica inclusions. The interface energies are approximately: $\gamma = 1.14$ J/m^2, $\gamma_I = 0.5$ J/m^2. $\gamma_B = 0.55$ J/m^2.[16] The angles α, β and μ

$$\gamma_s = 550 \ \text{ergs/cm}^2$$
$$\gamma = 1140 \ \text{ergs/cm}^2$$
$$\gamma_I = 500 \ \text{ergs/cm}^2$$
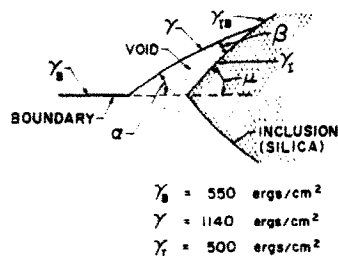
γ_{IB} ergs/cm²	α°	β°	μ°	$(\alpha-\beta-\mu)^\circ$
500	76	90	56	110
1000	76	64	74	66
1070	76	60	76	60
1250	76	48	77	47
1370	76	40	78	38
1500	76	28	80	24
		TYPE A VOIDS		TYPE B VOIDS

FIG. 15. The angle and interface energy relationship for a copper polycrystal containing silica inclusions. Void nucleation is possible for $\beta < 40^\circ$ (Type A voids) and for $\alpha + \beta - \mu < 60^\circ$ (Type B voids).

are given in Fig. 15 for various values of γ_{IB}. From consideration of results in this section we conclude that nucleation of Type A voids is possible for $\beta < 40^\circ$ or for $\gamma_{IB} < 1.37 \ \text{J/m}^2$. Nucleation of Type B voids is possible for $(\alpha + \beta - \mu) < 60^\circ$ or for $\gamma_{IB} < 1.07 \ \text{J/m}^2$. These limits are good only for the set of creep conditions specified in this paper. The limits for other cases can be calculated.

7. SUMMARY AND DISCUSSION

The kinetics of stress induced nucleation and growth voids in a grain boundary has been analysed in detail. Particular attention has been given to voids forming at second phase particles since these appear to be the prime sites for nucleation in the grain boundary. The cogent results are:

(a) Three types of void configuration in clean boundaries and two types of configurations at second phase particles are possible. The geometrical properties of all the configurations can be described by similar general functions. General solutions for the nucleation and growth of these voids are therefore possible.

(b) An expression for time-to-fracture has been derived for growth by boundary diffusion when the number of voids remains constant. The results are extrapolated to include growth by volume diffusion. The early stage of void growth is the slowest and accounts for most of the time-to-fracture.

(c) Using classical nucleation theory, the nucleation of the voids has been calculated. The energy barrier

for nucleation is a sensitive function of the free surface energy and of the volume of the void of critical radius.

(d) A numerical procedure has been developed which gives the time-to-fracture when nucleation and growth occur continuously and simultaneously.

(e) The time-to-rupture curves have been obtained for the case when a polycrystal is deformed at a constant strain-rate at different temperatures. When no sliding of the boundaries is allowed then void nucleation is possible only when interface energies are comparable to the total surface energy of the void being created. These conditions may be met at non-wetting or almost non-wetting inclusions.

(f) Stress concentrations are produced when sliding occurs in a boundary which contains inclusions. Upper bounds for these stresses are calculated and new time-to-fracture curves are obtained. Inclusions now become probable nucleation sites. Quantitative results are derived in terms of all the surface energies involved in the nucleation process.

(g) The time-to-fracture vs temperature curves show a minimum ductility at approximately $0.5T_M$. This is in agreement with the published experimental work.[2,3,17]

(h) The time-to-fracture curves shift with change in strain-rate, grain size, inclusion size, inclusion density and the distribution of the second phase. For results see Figs. 10–14.

(i) When no sliding is allowed the number of nuclei increase continuously with time but when stress concentrations due to sliding are taken into account then nucleation is catastrophic i.e. full nucleation occurs in the early stages of creep. Experimental work in support of the first[1,18] as well as the second process[6,19] is found in the literature.

(j) The results are applied to a copper polycrystal of grain size 10 μm being strained at 10^{-4} sec and containing silica inclusion of size 1 μm dispersed at a density of $10^{10}/\text{m}^2$ in the boundaries.

REFERENCES

1. R. T. RATCLIFFE and G. W. GREENWOOD, *Phil. Mag.* **12**, 59 (1965).
2. G. D. BENGOUGH, *J. Inst. Met.* **7**, 123 (1912).
3. F. N. RHINES and P. J. WRAY, *Trans. ASM* **54**, 117 (1961).

4. M. V. SPEIGHT and J. E. HARRIS, Met. Sci. J. 1, 83 (1967).
5. D. HULL and D. E. RIMMER, Phil. Mag. 4, 673 (1959).
6. P. R. OLIVER and L. A. GIRIFALCO, Acta Met. 10, 765 (1962).
7. J. E. HARRIS, Trans. Met. AIME 233, 1509 (1965).
8. P. J. CLEMM amd J. C. FISHER, Acta Met. 3, 70 (1955).
9. R. RAJ and M. F. ASHBY, Trans. Met. AIME 2, 1113 (1971).
10. P. G. SHEWMON, Diffusion in Solids, Chapter 2. McGraw-Hill, New York (1963).
11. M. F. ASHBY, Acta Met. 20, 887 (1972). Microstructure and design of alloys. Proc. 3rd Int. Conf. Strength of Metals and Alloys. Vol. 2, p. 8 (1973).
12. H. J. FROST and M. F. ASHBY, Harvard University Rept. A second report on deformation mechanism maps (August 1973).
13. R. RAJ and M. F. ASHBY, Trans. Met. AIME 3, 1937 (1972).
14. D. M. R. TAPLIN and V. N. WHITTAKER, J. Inst. Met. 92, 426 (1963-64); P. K. VENKITERSWARAN, D. C. FERGUSON and D. M. R. TAPLIN, Presented at Met. Soc. of AIME Fall Meeting at Detroit, Michigan, (October 1971).
15. G. J. COCKS and D. M. R. TAPLIN, Scripta Met. 3, 623 (1969).
16. W. T. READ, Dislocations in Crystals, Chapter 13. McGraw-Hill, New York (1953).
17. B. J. REID and J. N. GREENWOOD, Trans. Met. AIME 12, 503 (1958).
18. G. W. GREENWOOD, Phil. Mag. 19, 423 (1969).
19. H. E. EVANS and J. S. WADDINGTON, Phil. Mag. 1075 (1969).
20. C. HERRING, J. appl. Phys. 21, 437 (1950).
21. R. RAJ. To appear in Met. Trans. (1975).

NOMENCLATURE

γ surface free energy per unit area of the matrix material

γ_B interface free energy per unit area of the matrix grain boundary

γ_I surface free energy of the inclusion

γ_{IB} interface free energy of the inclusion–matrix boundary

V total volume of the void

S total surface area of the void

B area of the grain boundary which the void occupies

F_v a function of energy angles which provides the void volume (equation 3a)

F_S a function of energy angles which provides the void surface area (equation 3c)

F_B a function of energy angles which provides the area B (equation 3c)

α energy angle as defined by equation (1)

β energy angle as defined by equation (4) (also a constant in the calculation of appendix II)

μ energy angle as defined by equation (5)

D_B grain boundary self-diffusion coefficient—its value for copper: $10^{-5} \exp(-24.8 \text{ kcal/mole}/RT)$ m²/sec

D_v lattice self-diffusion coefficient—its value for copper: $6.2 \times 10^{-5} \exp(-49.6 \text{ kcal/mole}/RT)$ m²/sec

δ boundary thickness—its value: 4×10^{-10} m

r radius of curvature of the void surface

r_B radius of curvature of the projection of the void in the grain boundary

$2l$ average spacing between the voids

A a fractional measure of the grain boundary area occupied by voids, defined by equation (10)

Ω atomic volume—for copper: 1.1×10^{-29} m³

σ_∞ external applied stress

σ_n local normal stress at the interface which is responsible for void nucleation

E Young's modulus—for copper: 12.7×10^4 MN/m²

G shear modulus—for copper: 4.2×10^4 MN/m²

r_c critical radius for void nucleation

ΔG_c free energy barrier to void nucleation

ρ void density of the number of voids per unit area in the grain boundary

ρ_{max} maximum number of possible nucleation sites per unit area

ρ_c number of critical nuclei per unit area

ρ_p number of inclusions per unit area of boundary

p_t time dependent probability of adding one vacancy to a nucleus of critical size

$\dot{\rho}$ nucleation rate of voids per unit area

t_r time to fracture in sec

$\dot{\varepsilon}$ strain rate

d grain size

$\dot{C}$ average sliding rate of a grain boundary

p diameter of the inclusion

T_n normal tractions in the grain boundary which cause growth

$\Delta\mu$ the excess chemical potential of the atoms in the boundary relative to the stress free state

J_B boundary flux of atoms

β net number of atoms leaving per unit volume of the grain boundary during the steady state growth of voids.

APPENDIX I

(a) *Properties of voids in inclusion free boundaries*

The $F(\alpha)$ functions in equation (2) for the three and four grain junctions are as follows (8).

Three grain junctions

$$F_v(\alpha) = 2\left[\pi - 2\sin^{-1}\left(\tfrac{1}{2}\csc\alpha\right) + \tfrac{1}{3}\cos^2\alpha(4\sin^2\alpha - 1)^{1/2} - \cos^{-1}\left(\frac{\cot\alpha}{\sqrt{3}}\right)\cos\alpha(3 - \cos^2\alpha)\right] \quad (A1.1)$$

and

$$F_s(\alpha) - 2\cos\alpha F_B(\alpha) = 3F_v(\alpha). \quad (A1.2)$$

Four grain junctions

$$F_v(x) = 8\left[\frac{\pi}{3} - \cos^{-1}\frac{\sqrt{2} - \cos\alpha \cdot (3 - A^2)^{1/2}}{A\sin x}\right]$$
$$+ A\cos\alpha[(4\sin^2\alpha - A^2)^{1/2} - A^2/\sqrt{2}]$$
$$- 4\cos\alpha(3 - \cos^2\alpha)\sin^{-1}\left(\frac{A}{2\sin\alpha}\right),$$

where

$$A = \tfrac{2}{3}[\sqrt{2}(4\sin^2\alpha - 1)^{1/2} - \cos\alpha], \quad (A1.3)$$

and where equation (A1.2) still connects the different F functions.

(b) *Exact expression for volume of a type B void*

The volume of the region shown in Fig. A1 is given by the following expression:

$$V = 2r^3(I_1 + I_2),$$

where

$$I_1 = \int_{\sin(\mu-\alpha)}^{L}\left\{(1 - x^2)\cos^{-1}\frac{Z}{\sqrt{1 - x^2}}\right.$$
$$\left. - Z\sqrt{1 - x^2 - z^2}\right\}dx,$$

and

$$I_2 = \int_{L}^{\sin\beta}(1 - x^2)\cos^{-1}\frac{\beta}{\sqrt{1 - x^2}}$$
$$\left. - \cos\beta\sqrt{\sin^2\beta - x^2}\right\}dx, \quad (A1.4)$$

where

$$L = \frac{\cos\alpha - \cos\beta\cos\mu}{\sin\mu}$$

and

$$Z = \frac{\cos\alpha - x\sin\mu}{\cos\mu}.$$

The integral was evaluated numerically.

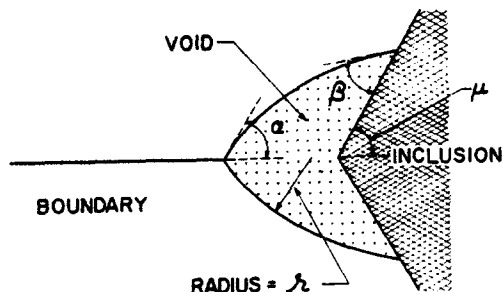FIG. A1. Evaluation of volume of a Type B void.

Time-to-Fracture: Fixed Number of Nuclei

(a) *Steady state void growth rate*

Let $T_n(R)$ be the normal tractions in the grain boundary in Fig. 3. The excess chemical potential of atoms in the boundary relative to the stress free state is[20]

$$\Delta\mu = -T_n\Omega. \quad (A2.1)$$

The transport equation for boundary diffusion is:

$$\mathbf{J}_B = -\frac{D_B}{\Omega kT}\nabla(\Delta\mu) \quad (A2.2)$$

The steady-state condition is that all parts of the boundary must give up or add the same amount of material, i.e.

$$\nabla \cdot \mathbf{J}_B = \beta, \quad (A2.3)$$

where β is a constant and is equal to the number of atoms removed per unit volume of the boundary which is thought of as having a thickness δ. These equations lead to the differential equation

$$\nabla^2(\Delta\mu) = -\frac{\beta kT\Omega}{D_B} \quad (A2.4)$$

which must be solved (in polar coordinates with circular symmetry) subject to the boundary conditions:

$$\frac{\partial\Delta\mu}{\partial R} = 0, \quad \text{at} \quad R = l, \quad (A2.5a)$$

and

$$\Delta\mu = -\frac{2\gamma\Omega}{r}, \quad \text{at} \quad R = r_B. \quad (A2.5b)$$

The answer is:

$$\Delta\mu = -\frac{\beta kT\Omega}{4D_B}(R^2 - r_B^2)$$
$$- \frac{\beta kT\Omega l^2}{2D_B}\log_e\frac{r_B}{R} - \frac{2\gamma\Omega}{r}. \quad (A2.6)$$

The condition of mechanical equilibrium requires that:

$$\pi l^2\sigma_\infty = \int_{r_B}^{l}T_n(R)2\pi R\,dR. \quad (A2.7)$$

Substituting equations (A2.1 and A2.6) in (A2.7) gives an expression for β. Since the growth rate of the void is equal to the amount of material added in the grain boundary, we have:

$$\frac{dV}{dt} = -\beta\delta\pi l^2\Omega\left(1 - \frac{r_B^2}{l^2}\right). \quad (A2.8)$$

Substitution of β leads to the final result given in equation (8).

(b) Calculation of time-to-fracture

Using the definition for $A(t)$ given in equation (10) and recalling from equations (2) that

$$r_B{}^2 = \frac{r^2}{\pi} F_B(\alpha) \qquad (A2.9a)$$

and

$$V = r^3 F_\Gamma(\alpha), \qquad (A2.10a)$$

equation (8) can be re-written in the following form:

$$\frac{dA}{dt} = \frac{32}{3\sqrt{\pi}} \frac{\Omega D_B \delta}{kT} \sigma_\infty \rho^{3/2} \frac{F_B^{3/2(\alpha)}}{F_v(\alpha)} f(A). \quad (A2.11)$$

where

$$f(A) = \frac{(1 - A)}{\sqrt{A}}$$

$$\times \frac{\{1 - (r_c/r)(1 - A)\}}{\frac{1}{2}\log_e 1/A - \frac{3}{4} + A(1 - A/4)}. \quad (A2.12)$$

Here r_c is the critical radius given by:

$$r_c = \frac{2\gamma}{\sigma_\infty} \qquad (A2.13)$$

and ρ is the number of voids per unit area of the boundary: $\rho = 1/(2l)^2$. Equation (A2.11) leads to an expression for time to fracture, t_r:

$$t_r = \frac{3\sqrt{\pi}}{32} \frac{kT}{\Omega D_B \delta} \frac{1}{\sigma_\infty \rho^{3/2}} \frac{F_v(\alpha)}{F_B^{3/2}(\alpha)} \int_{A_{\min}}^{A_{\max}} \frac{dA}{f(A)}. \quad (A2.14)$$

The integral in equation (A2.14) has been evaluated where the voids start to grow from critical size (A2.13). Its value, for $r_c = 100\,\text{A}^\circ$, and for a variable upper limit. is shown in Fig. A2. It is evident that the early stages of void growth are the slowest. The integral becomes relatively insensitive to $A_{\max}$ after $A_{\max} > 0.1$. In all computations in this paper we assume $A_{\max} = 0.5$ for which the integral is equal to 0.06.

The integral is also insensitive to the value of $A_{\min}$, defined by:

$$A_{\min} = \frac{r^2 F_B(\alpha)\rho}{\pi}. \qquad (A2.15)$$

This can be seen from Fig. A2, in which a variation of ρ (and thus of $A_{\min}$) by a factor of 10^8 makes little difference to the value of the integral.
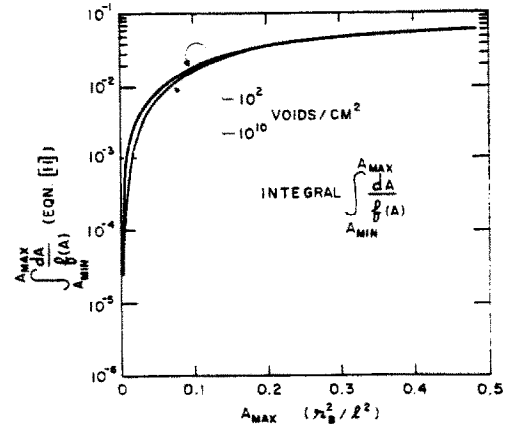

FIG. A2. The change in time-to-fracture (the integral is proportional to it) with α for two grain junctions.

APPENDIX III

Nucleation and Growth of Voids: A Computer Model

A computer model was developed to simulate the continuous nucleation and growth of voids in the grain boundary. Simultaneous nucleation and growth was assumed to occur at a constant rate during small, but discreet, time intervals Δt_x where the subscript determines the sequence of the time intervals. The radius of a void, r_{ij}, in the jth period depends upon the ith period during which it was born. The number of nuclei of radius r_{ij}, $\Delta\rho_i$ will be given by:

$$\Delta\rho_i = \dot{\rho}_i \Delta t_i \qquad (A3.1)$$

where $\dot{\rho}_i$ is given by equation (18). When all the nucleation sites, $\rho_{\max}$, have been exhausted, the nucleation rate goes to zero. New nuclei are assigned the critical radius (equation A2.13).

The computer simulation operates using equations (8 and 2). At every time step the fractional grain boundary interface which has been replaced by voids is calculated according to:

$$A_j = \Delta\rho_i r_{ij}{}^2 F_B(\alpha). \qquad (A3.2)$$

The value of j, for which $A_j \geq 0.5$, is determined and the time to fracture is then equal to $\sum_{k=1}^{i} \Delta t_k$. If the value of j is less than 25, Δt is decreased until $j > 25$. Increasing the minimum value of j from 25 to 50 increased the accuracy by only 10 per cent whereas the computer time needed for the calculation increased logarithmically.

At two-, three- and four-grain junctions, $\rho_{\max}$ was set equal to

$$\frac{1}{(\bar{r}_c{}^2 F_B(\alpha))} \; ; \quad \frac{1}{(\bar{r}_c d F_B^{1/2}(\alpha))} \; ; \quad \text{and} \quad \frac{2}{d^2}$$

respectively. Here d is the grain size, and $\bar{r}_c$ is the radius of a nucleus equal to the volume sum of the critical nucleus plus one atomic volume.

$\rho_{\max}$ was taken to be equal to $(p^2 \rho_p / b^2)$ when inclusions were present, p is the inclusion size and ρ_p the inclusion density in the grain boundary. However, for inclusions, all the nucleation sites were considered to be exhausted when the total number of nuclei was equal to the number of inclusions. The stress in equation (18) was assigned an upperbound value of 2.0×10^3 MN/m² which was assumed to be the ideal fracture strength of the interface.

CORRECTION TO: "INTERGRANULAR FRACTURE AT ELEVATED TEMPERATURE"

R. Raj, H. M. Shih and H. H. Johnson

Department of Materials Science and Engineering
Bard Hall, Cornell University
Ithaca, New York 14853

Introduction

An analysis for the growth of an array of cavities in a grain boundary by diffusive transport of vacancies was presented in an earlier paper (1). The paper dealt with the general problem of nucleation and growth of cavities in the grain boundary. We wish here to comment only upon that aspect of the calculation which pertains to the growth cavities under the influence of an applied tensile stress across the grain boundary or under the influence of internal gas pressure in the cavity. In this calculation the number of cavities per unit area of the grain boundary remains fixed (Section 3 and Appendix II in Ref. 1).

As described in Ref. 1, the volumetric growth rate of the cavity, dV/dt, is determined by using the diffusion equation (Eq. A2.2), the compatability equation for quasi-steady-state growth of the cavities (Eq. A2.3), and the equilibrium equation (Eq. A2.6), and by applying the appropriate boundary conditions (A2.5). The result is an expression for dV/dt by the boundary diffusion mechanism (Eq. 8), upon suitable integration of which an expression for time-to-fracture, t_r, is obtained (Eq. 11).

Correction

A mistake was made in the equation for mechanical equilibrium in the original paper (Eq. A2.7). The correct version is:

$$\pi \ell^2 \sigma_\infty + (p - \frac{2\gamma}{r}) \pi r_B^2 = \int_{r_B}^{\ell} T_n(R) 2\pi R dR \qquad (C1)$$

Here T_n is the normal traction across the grain boundary, σ_∞ is the remote applied tensile stress and ℓ and r_B are shown in the Fig. 1 which is repeated from the original paper and included here for convenience. In Eq. (A2.7) the second term on the left hand side of Eq. (C1) had been omitted. It arises from the fact that if an internal gas pressure is present inside the cavity, it produces a tensile force across the boundary which is equal to p, the pressure, times the area projected by the cavity at the boundary πr_B^2. Similarly, surface tension also produces normal stress on the surface of the cavity. The direction of this normal stress is in the opposite sense to the applied tensile stress since surface tension strives to close the cavity by sintering and is, therefore, equivalent to an applied compressive stress. The total magnitude of the surface tension force will be equal to the normal stress due to surface tension $2\gamma/r$ times πr_B^2 where γ is the surface tension and r is the radius of curvature of the cavity surface.

Fig. 1
The geometrical arrangement of the array of cavities within grain boundary (1).

Correction in the Expression for Time-To-Fracture

Following the same procedure as in Ref. 1, but using as one of the boundary conditions $\Delta\mu = (p - \frac{2\gamma}{r})\Omega$ at $R = r_B$ instead of Eq. (A2.5b), we get the following expression for the volumetric growth rate of the cavities which replaces Eq. 8* of Ref. 1:

$$\frac{dV}{dt} = 2\pi\Omega \, \frac{D_B}{kT} \, \frac{(\sigma_\infty + p - \frac{2\gamma}{r})(1 - \frac{r_B^2}{\ell^2})}{\ln\frac{\ell}{r_B} - \frac{3}{4} + \frac{r_B^2}{\ell^2}(1 - \frac{r_B^2}{4\ell^2})} \qquad (C2)$$

Once again, as before, we use the appropriate geometrical properties of the cavities (Eqs. 2 and 3), and then integrate Eq. (C2) to obtain an expression for time to fracture:

$$t_r = \frac{3\sqrt{\pi}}{32} \, \frac{kT}{\Omega D_B} \, \frac{1}{(\sigma_\infty + p)\rho^{3/2}} \, \frac{F_V(\alpha)}{F_B^{3/2}(\alpha)} \int_{A_{min}}^{A_{max}} \frac{dA}{f(A)} \qquad (C3)$$

where the correct version of the function $f(A)$ is given by:

$$f(A) = \frac{(1 - \frac{r_c}{r})(1 - A)}{\sqrt{A}\,[\frac{1}{2}\ln\frac{1}{A} - \frac{3}{4} + A(1 - A/4)]} \qquad (C4)$$

which differs slightly from the original equation (Eq. A2.12). In Eqs. (C2 - C4), D_B is the grain boundary self diffusion coefficient, δ is the boundary thickness, Ω is the atomic volume and ρ is the number of cavities per unit area of the grain boundary, i.e., $\rho = (2\ell)^{-2}$. $F_V(\alpha)$ and $F_B(\alpha)$ are the shape functions of the cavity which give the volume of the cavity and the area projected by the cavity at the boundary when multiplied by r^3 and r^2 respectively, r being the radius of curvature of the void surface. 2α is the angle subtended by the cavity of an equilibrium shape at the grain boundary so that $\cos\alpha = \gamma_B/2\gamma$ where γ_B is the grain boundary energy. The parameters r_c and A in Eqs. (C3) and (C4) are defined as:

$$A = \frac{r_B^2}{\ell^2} = 4r_B^2\rho = \frac{4r^2 F_B(\alpha)}{\pi}\rho$$

and $(C5)$

$$r_c = \frac{2\gamma}{\sigma_\infty + p}\quad.$$

The difference in the result for time to fracture as compared to the original equation would arise from the difference in the integral in Eq. (C3). A correction factor can be expected since the function $f(A)$ being integrated in Eq. (C4) differs somewhat from Eq. (A2.12). The result from the integration in Ref. 1 is shown as a solid line in Fig. II. The significant result was that the integral increases rapidly at first and then slowly approaches a saturation value of about 0.06. The result was shown to be insensitive to the choice of ρ and r_c. We will

---

* There was in fact a misprint in Eq. 8 in Ref. 1: the term $(\sigma_\infty - \frac{2\gamma}{r})(1 - \frac{r_B^2}{\ell^2})$ should have read as: $\sigma_\infty - \frac{2\gamma}{r}(1 - \frac{r_B^2}{\ell^2})$. In Eq. A2.12, which follows from Eq. 8, there was no error as a result of the misprint. The complete Eq. (8) was as follows:

$$\frac{dV}{dt} = 2\pi\Omega \, \frac{D_B}{kT} \, \frac{[\sigma_\infty - \frac{2\gamma}{r}(1 - \frac{r_B^2}{\ell^2})](1 - \frac{r_B^2}{\ell^2})}{\ln\frac{\ell}{r_B} - \frac{3}{4} + \frac{r_B^2}{\ell^2}(1 - \frac{r_B^2}{4\ell^2})}\quad.$$
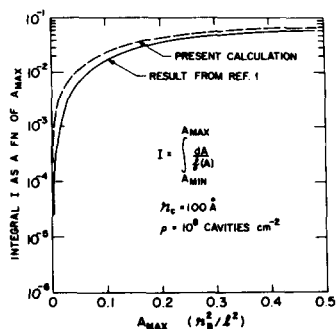
Fig. 2

Calculation of the integral in the expression for time-to-fracture, equation (C3). The result from Ref. 1 (solid line) is compared to the new result.

now calculate this integral for the new function $f(A)$ in Eq. (C4) and compare it to the original result.

The value for A_{min} in the new integration was determined in the following manner. First a value for r_C was assumed. From this the volume of the cavity was calculated. The volume of the critical cavity was increased by one atom volume to make it supercritical and the radius of the slightly larger cavity was used to calculate A_{min}. The new integration curve for increasing values of A_{max} is shown as a dashed line in Fig. II. The comparison is carried only up to $A_{max} = 0.5$ since the curve in Ref. 1 was limited to this value.

The interesting point in the comparison shown in Fig. II is that the early growth of cavities in the correct version is slower by about a factor of ten as compared to the original result, although the asymptotic value differs by only a small factor. This result

becomes clear upon comparing the net driving force for the growth of cavities in Eqs. (C2) and

(8). In Eq. (C2) it is $\sigma_\infty + p - \frac{2\gamma}{r}$ whereas in Eq. (8)* it was $\sigma_\infty + (p - \frac{2\gamma}{r})(1 - \frac{r_B^2}{\ell^2})$. The surface tension term, $\frac{2\gamma}{r}$, is stronger in Eq. (C2) since in Eq. (8) it is weighted by a factor which is less than unity. The influence of surface tension on cavity growth decreases as the cavity radius increases. We would expect, therefore, that the correction in the surface

tension term from $\frac{2\gamma}{r}$ to $\frac{2\gamma}{r}(1 - \frac{r_B^2}{\ell^2})$ would have a large effect only on the early growth of cavities as is shown quantitatively in Fig. II.

The correction in the expression for the time-to-fracture arises from the change in the value of the integral in Eqs. (C3) and (C4). In Ref. 1 the value of this integral was given to be 0.06; we shall call it I_{old}. The old value was evaluated for $A_{max} = 0.5$ on the assumption that when cavities have grown to a size where they occupy half the grain boundary area, the cavities would coalesce rapidly by plastic flow and failure would occur catastrophically. Although this point of instability will depend upon the nominal stress applied to the sample, we have found in fracture experiments with bicrystals that cavities can grow by diffusion until they nearly touch before fracture occurs (2). We assume, therefore, a value of 0.8 for A_{max}, i.e., $(r_B/\ell) = 0.9$, for calculating the new value of the integral, I_{new}. It should be noted that the magnitude of the integral does not depend critically on the choice of A_{max} as long as A_{max} is chosen to be greater than 0.2; this becomes clear from inspection of Fig. II.
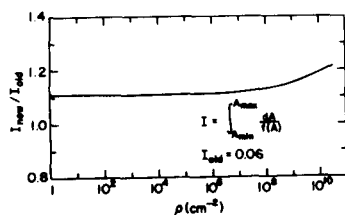

Fig. 3

The correction factor in the magnitude of the integral.

In view of the foregoing discussion the correction factor in the expression for time-to-fracture can be obtained by calculating the ratio of the integrals, I_{new}/I_{old}. The ratio was evaluated for different values of ρ. The result is given in Fig. 3. The correction factor is not large; it varies from 1.1 to 1.2 depending on the value for ρ. It is interesting that whereas in the earlier calculation the value of the integral was essentially independent of ρ, it is now sensitive to values of ρ greater than 10^7 cm^{-2}.

---

* In Ref. 1, it had been assumed that $p = 0$.

Results

(a) Time-to-Fracture

The correct experssion for time-to-fracture is obtained by substituting the value for the integral in Eq. (C3). It follows from the above discussion that a reasonable value for the integral would be 0.072, i.e., 1.2 x 0.06 which leads to:

$$t_r = 0.0012 \frac{kT}{(\sigma_\infty + p)\Omega} \cdot \frac{1}{\delta D_B \rho^{3/2}} \frac{F_v(\alpha)}{F_B^{3/2}(\alpha)} \quad . \qquad (C6)$$

For cavities growing in two grain junctions the function $F_v(\alpha)/F_B^{3/2}(\alpha)$ can be calculated using the expressions given in Eqs. (2 and 3) of Ref. 1. For pure metals with clean surfaces it is reasonable to assume that $\gamma_B \approx \gamma/2$ which leads to $\alpha \approx 75°$. Substituting this value in Eq. (C6) leads to

$$t_r = .006 \frac{kT}{(\sigma_\infty + p)\Omega} \cdot \frac{\lambda^3}{\delta D_B} \qquad (C7)$$

where we have substituted $\rho = 1/\lambda^2$ where λ is the average spacing of the cavities in the boundary. Note that $\lambda = 2\ell$.

(b) Early Growth of Cavities

In some applications it may be useful to be able to calculate the rate of growth of cavities before fracture. This information is contained in Fig. 2. The exact numbers from the integration using $r_c = 25$ Å are given in Table I for two different values of ρ. Here we have calculated the time required for the cavities to grow until they occupy an area fraction, A_{max}, in the boundary. The time required to reach A_{max}, i.e., $t(A_{max})$ is normalized according to Eq. (C7) and calculated in Table I.

TABLE I

A_{max}	$t(A_{max})/\{\frac{kT}{(\sigma_\infty + p)} \cdot \frac{\lambda^2}{\delta D_B}\}$	
	$\rho = 10 \text{ cm}^{-2}$	$\rho = 10^9 \text{ cm}^{-2}$
10^{-3}	5.4×10^{-6}	6.0×10^{-5}
10^{-2}	1.0×10^{-4}	1.5×10^{-4}
10^{-1}	1.5×10^{-3}	1.7×10^{-3}
0.8	5.5×10^{-3}	6.0×10^{-3}

Discussion

The equation for force equilibrium in the analysis of quasi-steady-state growth of an array of cavities in the grain boundaries was incorrect in Ref. 1. Use of the correct equation leads to a small correction factor ranging from 1.1 to 1.2, in the expression for time-to-fracture. The correction, however, has a strong influence on the rate of growth of cavities when the cavities are small and comparable to the critical size. In this instance the correction factor is about 10. In each case the correction leads to a retardation in the growth rate of cavities. The reason for this is that the contribution of surface tension in the driving force for cavity growth had been underestimated in the original calculation. Since surface tension opposes cavity growth, the earlier calculation was overestimating the driving force for cavity growth.

References

1. R. Raj and M. F. Ashby, Acta Met., 23, 653 (1975).

2. R. Raj, "Intergranular Fracture in Bicrystals", Materials Science Center Report #2842, Cornell University, Ithaca, NY, May 1977.